

## Fluorescence

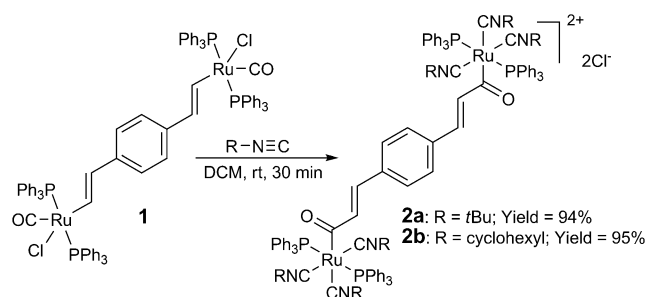
# Off/On Fluorescent Chemosensors for Organotin Halides Based on Binuclear Ruthenium Complexes\*\*

Yufen Niu, Feifei Han, Qian Zhang, Tingwan Xie, Liu Lu, Shunhua Li,\* and Haiping Xia\*

Fluorescent chemosensors (FCS), which can selectively recognize guest species, offer an essential strategy for real-space and real-time monitoring or imaging.<sup>[1]</sup> Design of high-performance FCS for biologically or environmentally important species is a topic attracting considerable attention in supramolecular chemistry. During the past few decades, numerous FCS have been developed based on molecular recognition through noncovalent interactions (e.g., hydrogen bonding in anion recognition,<sup>[2]</sup> metal–ligand interaction in sensing, for example, metal cations<sup>[3]</sup> or gaseous species<sup>[4]</sup>). Halogen bonding (XB)—the interaction based on donation of electron density from a Lewis base to an electron-deficient halogen atom—is a frequently occurring noncovalent interaction parallel to hydrogen bonding in molecular self-assembly processes.<sup>[5]</sup> However, XB has so far mostly been studied *in silico* and in solid state,<sup>[5a]</sup> and solution-phase molecular sensing through XB remains largely unexplored. The first and only two examples of XB-based FCS were reported recently by Beer's group, both of which used macrocyclic halo-imidazolium receptors to recognize halide anions through charge-assisted XB in solution.<sup>[6]</sup> Compared with anions, common neutral Lewis bases are more intriguing XB acceptors in the construction of XB receptors for halogenated organic compounds. Many important environmental pollutants including polychlorinated biphenyls, dioxins and some toxic organometallics are halogen-abundant compounds while efficient FCS for these species are still unavailable. Herein, we report a design of off/on fluorescent chemosensors for organotin halides based on XB in solution.

Organotin compounds (OTCs) are known for their wide distribution and strongly toxic effect on marine organisms.<sup>[7]</sup> OTCs are represented by the formula  $R_n\text{SnX}_{(4-n)}$ , where Sn is the tin atom, R is an alkyl or aryl group, X is usually a halide

or hydroxide anion, and  $n$  ranges from 1 to 4. The degradation products of OTCs usually exist as di- or mono-organotin complexes,<sup>[8]</sup> both with high biological activities.<sup>[9]</sup> For studying the toxicology of OTCs, we have reported the first FCS for hydroxylated organotin.<sup>[10]</sup> Further effort was made to develop FCS for organotin halides by taking advantage of the XB activities of these species. Many percyanometallates were reported to be efficient XB acceptors.<sup>[5b,11]</sup> This enlightened us to synthesize binuclear ruthenium complexes **2a** and **2b** (Scheme 1), which contain two percyanometallate-based



Scheme 1. Synthesis of the binuclear ruthenium complexes.

binding sites bridged by a 1,4-phenylenediacryl fluorophore, as the fluorogenic receptors. Both **2a** and **2b** were characterized by means of NMR (<sup>1</sup>H, <sup>13</sup>C, and <sup>31</sup>P) spectra and high-resolution mass spectra. The structure of **2b** has been confirmed by X-ray diffraction (Figure 1).

The optical responses of the synthesized receptors to OTCs were tested first in dichloromethane. The solution of **2a** turns red immediately after addition of  $\text{PhSnCl}_3$ . As shown in Figure 2 A, addition of  $\text{PhSnCl}_3$  results in a decrease of the low-energy absorption of **2a** ( $\lambda_m = 345 \text{ nm}$ ) characteristic of

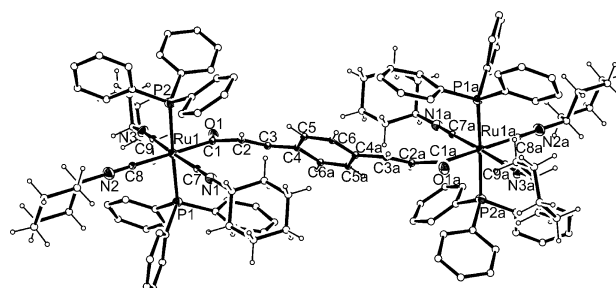


Figure 1. Molecular structure for the cation of **2b**. The counter anions and some of the hydrogen atoms are omitted for clarity. Symmetry transformations used to generate equivalent atoms:  $-x+2$ ,  $-y+2$ ,  $-z+2$ .

[\*] Y. Niu, Q. Zhang, L. Lu, Dr. S. Li

Department of Chemistry and Key Laboratory of Analytical Sciences  
College of Chemistry and Chemical Engineering, Xiamen University  
Xiamen 361005 (P.R. China)  
E-mail: lishua@xmu.edu.cn

F. Han, T. Xie, Prof. H. Xia

State Key Laboratory of Physical Chemistry of Solid Surfaces  
College of Chemistry and Chemical Engineering, Xiamen University  
Xiamen, 361005 (P.R. China)  
E-mail: hpxia@xmu.edu.cn

[\*\*] This work was supported by the National Basic Research Program of China (grant number 2011CB910403), the National Natural Science Foundation of China (grant numbers 21175113, 20925208, and 20835005), and the Fundamental Research Funds for the Central Universities (grant number 2011121015).

Supporting information for this article is available on the WWW under <http://dx.doi.org/10.1002/ange.201209549>.

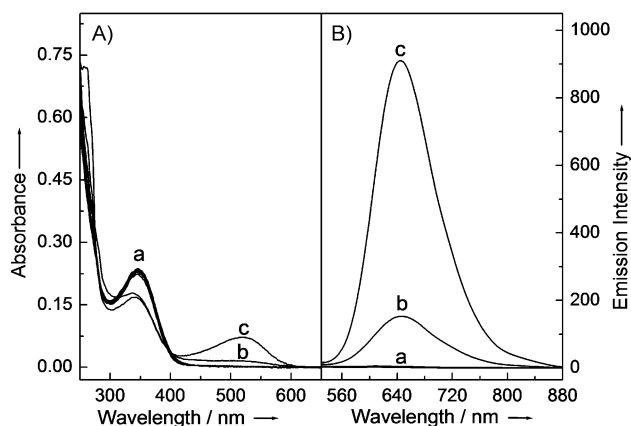


**Figure 2.** A) Absorption and B) photoluminescence spectra of **2a** (10  $\mu\text{M}$ ) in dichloromethane in the presence of different organotin species (50  $\mu\text{M}$ ): a) blank or other compounds including  $\text{Bu}_2\text{SnCl}_2$ ,  $\text{Bu}_3\text{SnCl}$ ,  $\text{Bu}_4\text{Sn}$ ,  $\text{MeSnCl}_3$ ,  $\text{Me}_2\text{SnCl}_2$ ,  $\text{Ph}_2\text{SnCl}_2$ ,  $\text{Ph}_3\text{SnCl}$ ,  $\text{Me}_3\text{SnBr}$ ,  $\text{Et}_3\text{SnBr}$ ,  $\text{Bu}_3\text{SnBr}$  and  $\text{Me}_2\text{SnBr}_2$ , b)  $\text{BuSnCl}_3$  and c)  $\text{PhSnCl}_3$ . The emission spectra were recorded upon excitation at 510 nm.

a  $\pi \rightarrow \pi^*$  transition of the 1,4-phenylenediacryl chromophore<sup>[12]</sup> and the onset of a new long-wavelength absorption band ( $\lambda_{\text{m}} = 518 \text{ nm}$ ). The remarkable red shift of low-energy absorption band indicates that the double-headed receptor molecules may be linked to form “J”-type aggregates of the chromophores.<sup>[13]</sup> Dynamic light scattering experiments revealed that aggregates with diameters larger than 500 nm were formed in the  $\text{PhSnCl}_3$ -titrated solutions of **2a** (see Figure S4 in the Supporting Information). Accompanying the absorption response, intense red luminescence ( $\lambda_{\text{em}} = 645 \text{ nm}$ ) was observed in the  $\text{PhSnCl}_3$ -titrated solution while the blank solution of **2a** was non-luminescent upon excitation at 510 nm at room temperature (Figure 2B). In accord with the assignment of the new absorption band, the aggregate-dominated long-wavelength emission showed a short lifetime of 0.77 ns (Figure S11). When excess  $\text{PhSnCl}_3$  was added, the photoluminescence quantum yield ( $\varphi_{\text{F}}$ ) of **2a** rose to 0.29, which is more than 3000 times higher than that in the absence of OTCs (Figure S12). Addition of  $\text{BuSnCl}_3$  resulted in similar yet less sensitive absorption and fluorescence responses while no obvious spectral changes were observed upon addition of other investigated OTCs, halogenated hydrocarbons (e.g. 1,4-dichloro-2-butene and 1,3-dichlorobenzene) or tetraalkylammonium halides. The obviously higher affinity of **2a** for  $\text{PhSnCl}_3$  than that for  $\text{BuSnCl}_3$  is proposed to result from the assistance of  $\pi$ - $\pi$  interactions between the phenyl group of  $\text{PhSnCl}_3$  and the  $\text{PPh}_3$  ligands of **2a** in binding the OTC guests.

The remarkable  $\varphi_{\text{F}}$  increase induced by  $\text{PhSnCl}_3$  can be interpreted in terms of “aggregation-induced emission” (AIE).<sup>[14]</sup> In the absence of OTCs, the random vibration and/or rotation of the multifurcate  $\text{PPh}_3$  and alkyl isocyanide ligands greatly facilitates the non-irradiative decay of the excited molecules of **2a** ( $\lambda_{\text{em}} = 511 \text{ nm}$ ), leading to the very low  $\varphi_{\text{F}}$  (Figure S8, Supporting Information). In the presence of OTCs, the binding-induced aggregation of **2a** results in not only a new luminescent electronic transition dominated by the J-aggregates but also a great enhancement in the rigidity of the fluorophores. Consequently, the intramolecular vibra-

tion or rotation of the fluorophores is significantly suppressed to give a high  $\varphi_{\text{F}}$  of the aggregate emission. It is believed that the bulky ligands of **2a** also play an important role in this process to sterically preclude the  $\pi$ - $\pi$  stacking of the fluorophores and the as-resulted fluorescence quenching. Interestingly, the OTC-induced aggregation of **2a** results in intense aggregate-dominated emission but not in enhanced monomer emission occurring in most of the reported AIE systems.<sup>[14,15]</sup> This noteworthy characteristics of **2a** supports the high target-to-background ratio of the fluorescence responses shown in Figure 2B.

The OTC binding mechanism underlying the AIE responses was studied. The strong triple infrared (IR) absorption bands of  $\text{PhSnCl}_3$  observed at 728, 691, and 442  $\text{cm}^{-1}$ , characteristic of the Sn-Cl bond stretching, were greatly weakened upon reaction with **2a**; meanwhile, the intense  $\text{N} \equiv \text{C}$  stretching absorption of **2a** at 2134  $\text{cm}^{-1}$  was also reduced markedly with a slight blue shift<sup>[16]</sup> (Figure S6). These observations suggest the formation of XBs involving the  $\text{N} \equiv \text{C}$  groups and the metal-bound halogen atoms in the reaction product. To confirm the important role of the XB-active percyanometallate moieties in the guest binding process, receptor **2b** was tested for a comparison with **2a**. **2b** displayed absorption and fluorescence behaviors similar to **2a** in the presence of OTCs (Figure S16). However, the binding affinity of **2b** for organotin trichlorides was lower than that of **2a** because of its larger steric hindrance. Since both percyanometallates and halometallates are able to form XBs with solvent molecules,<sup>[5b]</sup> different solvents were also tested as the sensing media. The spectral behaviors of **2a** or **2b** in trichloromethane are similar to those observed in dichloromethane. No spectral response has been observed when **2a** or **2b** was titrated with OTCs in lowly XB-active solvents such as ethanol or dioxane. However, when the solvent was changed from dichloromethane (XB donors) to acetonitrile (XB acceptors), the resulting responses to OTCs (Figure 3) were greatly different from those shown in Figure 2. All the investigated organotin halides induced

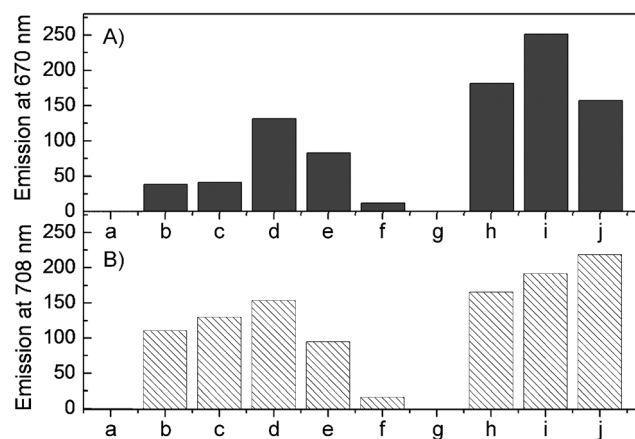


**Figure 3.** Fluorescence responses of A) **2a** and B) **2b** in acetonitrile to different organotin species (50  $\mu\text{M}$ ): a) blank, b)  $\text{Me}_2\text{SnCl}_2$ , c)  $\text{Bu}_2\text{SnCl}_2$ , d)  $\text{Ph}_2\text{SnCl}_2$ , e)  $\text{Ph}_3\text{SnCl}$ , f)  $\text{Bu}_3\text{SnCl}$ , g)  $\text{Bu}_4\text{Sn}$ , h)  $\text{PhSnCl}_3$ , i)  $\text{BuSnCl}_3$ , and j)  $\text{Me}_2\text{SnBr}_2$ . Concentration of **2a** or **2b**: 10  $\mu\text{M}$ . Excitation wavelength: **2a**, 527 nm; **2b**, 563 nm.

obvious red emission from **2a** or **2b** while no response was observed upon addition of  $\text{Bu}_4\text{Sn}$  which is not XB-active. Apparently, solvent molecules participate in the XB-driven guest binding process. It was therefore proposed that the receptor molecules were linked through the solvent-assisted XB interaction between the percyanometallate moieties and the metal-bound halogen atoms to form luminescent aggregates in the sensing reaction. Dependence on the assistance of solvent molecules makes the binding process changeable. As a consequence, no stable binding stoichiometry has been found in the sensing reaction, representing a case different from most coordination reactions (Figure S13).

The designed receptors were applied to the fluorescent detection of organotin halides. Figure 4 shows the fluorescence evolution of **2a** in dichloromethane upon titration with

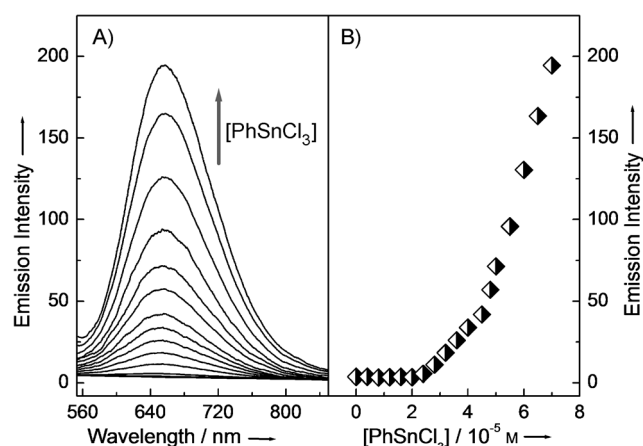


**Figure 4.** Emission behavior of **2a** (10  $\mu\text{M}$ ) in dichloromethane in the presence of increasing amount of  $\text{PhSnCl}_3$  upon excitation at 510 nm.

$\text{PhSnCl}_3$ . Interestingly, a multi-gradient response was observed. When less than two equivalents of  $\text{PhSnCl}_3$  were added, there was no obvious absorption or fluorescence change. Further increase in the OTC concentration led to the onset and gradual enhancement of the red fluorescence. After nearly five equivalents of  $\text{PhSnCl}_3$  were added, the emission enhancement was obviously accelerated. Variation of the initial concentration of **2a** resulted in similar fluorescence evolution profiles. These observations further characterize the XB interaction between the percyanometallate group and  $\text{PhSnCl}_3$  as a multi-molecule binding mode: each percyanometallate group of **2a** independently binds the first  $\text{PhSnCl}_3$  molecule while the second  $\text{PhSnCl}_3$  molecule is thermodynamically preferred to be shared with another binding site. As a consequence, more than two equivalents of  $\text{PhSnCl}_3$  should be added to induce the AIE response. At the beginning of aggregation, there are not enough guest molecules to inhibit the intramolecular vibration and/or rotation of the receptor molecules in aggregates through XB interaction, leading to lower  $\varphi_F$  of the aggregate-dominated emission. When the receptor molecules become more and more rigid in the guest binding process, further interacting with a target molecule will significantly restrict the intramolecular vibration and/or rotation of the receptor and therefore results in higher  $\varphi_F$ .

The proposed binding mode was supported by the NMR spectral traces of the  $\text{PhSnCl}_3$  sensing reactions (Figure 5). The characteristic  $^{31}\text{P}\{^1\text{H}\}$  NMR signal of **2a** was slightly shifted by two equivalents of  $\text{PhSnCl}_3$ . However, it was up-

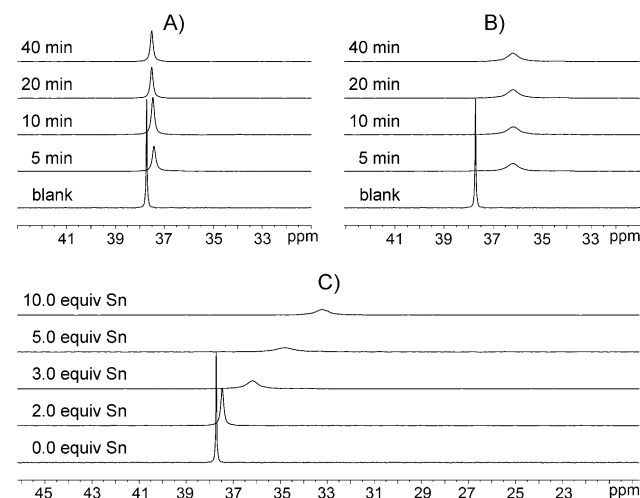


**Figure 5.**  $^{31}\text{P}\{^1\text{H}\}$  NMR spectral traces of **2a** in reactions with  $\text{PhSnCl}_3$  in  $\text{CD}_2\text{Cl}_2$ . Conditions: A)  $[\text{PhSnCl}_3] = 2.0$  [**2a**], B)  $[\text{PhSnCl}_3] = 3.0$  [**2a**], and C) reaction time = 10 minutes.

field shifted remarkably when the OTC concentration was further increased. Furthermore, the signal region was greatly broadened, indicating the involvement of **2a** in multiple binding ensembles because of aggregation. Based on the special signalling mechanism of **2a** described above, the receptors were pretreated with two equivalents of  $\text{PhSnCl}_3$  in the sensing solutions and then detection of  $\text{PhSnCl}_3$  at the micromolar level could be well established on a fluorophotometer. It should be pointed out that the  $\text{PhSnCl}_3$  sensing process was specially studied herein for the purpose of illuminating the signalling mode of the developed XB-based FCS. At most occasions of related analytical practices, the sensing system can be established in acetonitrile and applied to the visual detection of OTCs, which involves the extraction of OTCs by the organic solvent.

The  $\text{PhSnCl}_3$  sensing performance of **2a** was further evaluated in the presence of other OTCs. The variations of the  $\text{PhSnCl}_3$  sensing responses indicate that most of the organotin halides participates in the target binding process (Figure 6A). Obviously, all the investigated organotin halides are able to interact with percyanometallate receptors through XB. However, only the organotin trihalides are sterically able to link two percyanometallate receptors together in dichloromethane, resulting in the off/on fluorescence response selective for  $\text{PhSnCl}_3$  and  $\text{BuSnCl}_3$  over other investigated OTCs (Figure 2). The coexistence of other organotin chlorides causes minor interferences, indicating their remarkably lower binding affinity compared with that of  $\text{PhSnCl}_3$ . As a different case, coexistence of a high concentration of organotin bromides significantly reduces the fluorescence responses. The accompanying reduction of the aggregate-dominated absorption response (Figure S14) makes it clear that the involvement of organotin bromides in the XB binding

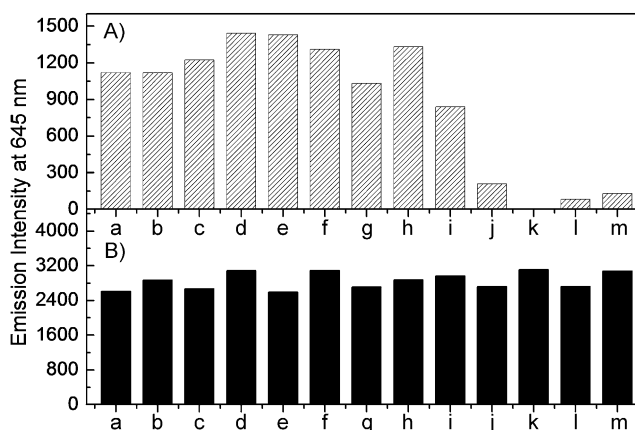


**Figure 6.** The influence of coexisting organotin species on the PhSnCl<sub>3</sub> sensing response of **2a** (10 μM) in dichloromethane upon excitation at 510 nm. Coexisting species: a) blank, b) Bu<sub>4</sub>Sn, c) Me<sub>2</sub>SnCl<sub>2</sub>, d) Bu<sub>2</sub>SnCl<sub>2</sub>, e) Ph<sub>2</sub>SnCl<sub>2</sub>, f) Bu<sub>3</sub>SnCl, g) Ph<sub>3</sub>SnCl, h) MeSnCl<sub>3</sub>, i) BuSnCl<sub>3</sub>, j) Me<sub>3</sub>SnBr, k) Et<sub>3</sub>SnBr, l) Bu<sub>3</sub>SnBr, and m) Me<sub>2</sub>SnBr<sub>2</sub>. Two concentration levels of PhSnCl<sub>3</sub> were investigated: A) 50 μM and B) 300 μM. All the coexisting species have the same concentration of 500 μM except for BuSnCl<sub>3</sub> (100 μM).

ensemble greatly counteracts the formation of J-aggregates of **2a**. Interestingly, the sensing responses are enhanced by Me<sub>2</sub>SnCl<sub>2</sub> or Bu<sub>3</sub>SnCl but greatly reduced by their bromide analogs, indicating a great difference between the steric effect of the XBs formed by organotin chlorides and that by their bromide analogs. Nevertheless, the different influences of the coexisting OTCs on the fluorescence responses were leveled in the presence of excess PhSnCl<sub>3</sub> (Figure 6B). The above observations indicate the remarkably higher affinity of **2a** for PhSnCl<sub>3</sub> over other OTCs in dichloromethane and thus validate the target recognition ability of the fluorogenic XB receptors.

In summary, XB-driven molecular recognition has been used to develop the first FCS for organotin halides. Chromophore-bridged binuclear ruthenium complexes containing multiple isocyanide ligands were synthesized as XB-active receptors with AIE characteristics. Interaction with organotin halides leads to aggregation of the receptor molecules in solution and the resulting off/on fluorescence responses in the near-infrared region. Visual detection of organotin halides at the micromolar concentration level can be easily carried out by the developed FCS. Our study confirms that cooperation of multiple XBs in solution is able to support high-affinity binding between small molecules. Furthermore, the monomer-to-aggregate conversion of chromophores, which usually results in high-contrast spectral changes, has proven to be a suitable signaling strategy for XB-motivated molecular sensing. Both the recognition and signalling mechanisms discussed herein are highly constructive for further designs of FCS targeting challenging species such as dioxins and dioxin-like polychlorinated biphenyls.

## Experimental Section

**2a:** A solution of *t*BuNC (0.40 mL, 3.50 mmol) was slowly added to a solution of complex **1** (391.6 mg, 0.26 mmol) in CH<sub>2</sub>Cl<sub>2</sub> (15 mL).

The reaction mixture was stirred for 30 minutes to give an orange solution. The volume of the mixture was reduced to about 1 mL under vacuum. Addition of diethyl ether (15 mL) to the residue produced an orange solid, which was collected by filtration, washed with diethyl ether, and dried under vacuum. Yield: 490.0 mg, 94%. <sup>1</sup>H NMR (CD<sub>2</sub>Cl<sub>2</sub>, 500.2 MHz): δ = 7.5–7.4 (m, 60H, PPh<sub>3</sub>), 6.6 (s, 4H, C<sub>6</sub>H<sub>4</sub>), 6.1 (d, <sup>3</sup>J(HH) = 15.5 Hz, 2H, RuCOCH), 5.4 (d, <sup>3</sup>J(HH) = 15.5 Hz, 2H, RuCOCH=CH), 1.1 (s, 18H, *t*Bu), 1.0 ppm (s, 36H, *t*Bu). <sup>31</sup>P{<sup>1</sup>H} NMR (CD<sub>2</sub>Cl<sub>2</sub>, 202.5 MHz): δ = 37.7 ppm (s, RuPPh<sub>3</sub>). <sup>13</sup>C{<sup>1</sup>H} NMR (CD<sub>2</sub>Cl<sub>2</sub>, 125.8 MHz): δ = 256.7 (br, RuCO), 149.4 (br, RuCN), 147.7 (br, Ru-CN), 139.6 (s, RuCOCH), 137.0 (s, *ipso*-C<sub>6</sub>H<sub>4</sub>), 134.7–128.8 (m, PPh<sub>3</sub>), 127.9 (s, C<sub>6</sub>H<sub>4</sub>), 125.3 (s, RuCOCH=CH), 58.5 (s, *t*Bu), 58.3 (s, *t*Bu), 30.1 (s, *t*Bu), 29.9 ppm (s, *t*Bu). HRMS (ESI) *m/z* for [C<sub>114</sub>H<sub>122</sub>N<sub>6</sub>O<sub>2</sub>P<sub>4</sub>Ru<sub>2</sub>]<sup>2+</sup>: calc. 967.3333 [*M*/2]<sup>+</sup>; found 967.3365 [*M*/2]<sup>+</sup> with expected isotopic distribution.

**2b:** A solution of cyclohexyl isocyanide (0.22 mL, 1.77 mmol) was slowly added to a solution of complex **1** (195.8 mg, 0.13 mmol) in CH<sub>2</sub>Cl<sub>2</sub> (10 mL). The reaction mixture was stirred for 30 minutes to give an orange solution. The volume of the mixture was reduced to about 1 mL under vacuum. Addition of diethyl ether (10 mL) to the residue produced a light pink solid, which was collected by filtration, washed with diethyl ether, and dried under vacuum. Yield: 266.9 mg, 95%. <sup>1</sup>H NMR (CD<sub>2</sub>Cl<sub>2</sub>, 500.2 MHz): δ = 7.5–7.3 (m, 60H, PPh<sub>3</sub>), 6.8 (s, 4H, C<sub>6</sub>H<sub>4</sub>), 6.6 (d, <sup>3</sup>J(HH) = 15.5 Hz, 2H, RuCOCH), 5.8 (d, <sup>3</sup>J(HH) = 15.5 Hz, 2H, RuCOCH=CH), 3.2–0.8 ppm (m, 66H, C<sub>6</sub>H<sub>11</sub>). <sup>31</sup>P{<sup>1</sup>H} NMR (CD<sub>2</sub>Cl<sub>2</sub>, 202.5 MHz): δ = 36.2 ppm (s, RuPPh<sub>3</sub>). <sup>13</sup>C{<sup>1</sup>H} NMR (CD<sub>2</sub>Cl<sub>2</sub>, 125.8 MHz): δ = 259.3 (br, RuCO), 151.1 (br, RuCN), 148.1 (br, Ru-CN), 140.5 (s, RuCOCH), 137.2 (s, *ipso*-C<sub>6</sub>H<sub>4</sub>), 135.0–128.8 (m, PPh<sub>3</sub>), 128.3 (s, C<sub>6</sub>H<sub>4</sub>), 125.8 (s, RuCOCH=CH), 55.5–23.6 ppm (m, C<sub>6</sub>H<sub>11</sub>). HRMS (ESI) *m/z* for [C<sub>126</sub>H<sub>134</sub>N<sub>6</sub>O<sub>2</sub>P<sub>4</sub>Ru<sub>2</sub>]<sup>2+</sup>: calc. 1045.3803 [*M*/2]<sup>+</sup>; found 1045.3851 [*M*/2]<sup>+</sup> with expected isotopic distribution.

Received: November 29, 2012

Revised: March 28, 2013

Published online: April 15, 2013

**Keywords:** fluorescent probes · ruthenium complexes · sensors · tin

- [1] a) A. W. Czarnik in *Fluorescent Chemosensors for Ion and Molecule Recognition*, American Chemical Society, Washington, DC, **1992**; b) D. W. Domaille, E.-L. Que, C.-J. Chang, *Nat. Chem. Biol.* **2008**, *4*, 168–175; c) T. Terai, T. Nagano, *Curr. Opin. Chem. Biol.* **2008**, *12*, 515–521.
- [2] a) R. M. Duke, E. B. Veale, F. M. Pfeffer, P. E. Kruger, T. Gunnlaugsson, *Chem. Soc. Rev.* **2010**, *39*, 3936–3953; b) T. Gunnlaugsson, M. Glynn, G. M. Tocci, P. E. Kruger, F. M. Pfeffer, *Coord. Chem. Rev.* **2006**, *250*, 3094–3117; c) R. Martínez-Máñez, F. Sancenón, *Chem. Rev.* **2003**, *103*, 4419–4476; d) L. Fabbri, M. Licchelli, G. Rabaioli, A. Taglietti, *Coord. Chem. Rev.* **2000**, *205*, 85–108.
- [3] a) M. Formica, V. Fusi, L. Giorgi, M. Micheloni, *Coord. Chem. Rev.* **2012**, *256*, 170–192; b) H. N. Kim, W. X. Ren, J. S. Kim, J. Yoon, *Chem. Soc. Rev.* **2012**, *41*, 3210–3244; c) L. Prodi, F. Bolletta, M. Montalti, N. Zaccaroni, *Coord. Chem. Rev.* **2000**, *205*, 59–83; d) B. Valeur, I. Leray, *Coord. Chem. Rev.* **2000**, *205*, 3–40.
- [4] a) S. E. Angell, C. W. Rogers, Y. Zhang, M. O. Wolf, W. E. Jones, *Coord. Chem. Rev.* **2006**, *250*, 1829–1841; b) C. W. Rogers, M. O. Wolf, *Coord. Chem. Rev.* **2002**, *233*–234, 341–350.
- [5] a) M. Erdélyi, *Chem. Soc. Rev.* **2012**, *41*, 3547–3557; b) R. Bertani, P. Sgarbossa, A. Venzo, F. Lelj, M. Amati, G. Resnati, T. Pilati, P. Metrangola, G. Terraneo, *Coord. Chem. Rev.* **2010**, *254*, 677–695; c) G. Cavallo, P. Metrangola, T. Pilati, G. Resnati, M. Sansotera, G. Terraneo, *Chem. Soc. Rev.* **2010**, *39*, 3772–3783;

- d) M. Fourmigué, *Curr. Opin. Solid State Mater. Sci.* **2009**, *13*, 36–45; e) P. Metrangolo, F. Meyer, T. Pilati, G. Resnati, G. Terraneo, *Angew. Chem.* **2008**, *120*, 6206–6220; *Angew. Chem. Int. Ed.* **2008**, *47*, 6114–6127; f) H. Wei, W. Jin, *Chinese J. Anal. Chem.* **2007**, *35*, 1381–1386; g) P. Metrangolo, H. Neukirch, T. Pilati, G. Resnati, *Acc. Chem. Res.* **2005**, *38*, 386–395; h) P. Metrangolo, G. Resnati, *Chem. Eur. J.* **2001**, *7*, 2511–2519.
- [6] a) A. Caballero, F. Zapata, N. G. White, P. J. Costa, V. Félix, P. D. Beer, *Angew. Chem.* **2012**, *124*, 1912–1916; *Angew. Chem. Int. Ed.* **2012**, *51*, 1876–1880; b) F. Zapata, A. Caballero, N. G. White, T. D. W. Claridge, P. J. Costa, V. Félix, P. D. Beer, *J. Am. Chem. Soc.* **2012**, *134*, 11533–11541.
- [7] a) C. Pellerito, L. Nagy, L. Pellerito, A. Szorcsik, *J. Organomet. Chem.* **2006**, *691*, 1733–1747; b) K. E. Appel, *Drug Metab. Rev.* **2004**, *36*, 763–786; c) V. C. Karpik, C. L. Eyer, *Cell Biol. Toxicol.* **1999**, *15*, 261–268.
- [8] a) B. A. Buck-Koehntop, F. Porcelli, J. L. Lewin, C. J. Cramer, G. Veglia, *J. Organomet. Chem.* **2006**, *691*, 1748–1755; b) S. K. Dubey, U. Roy, *Appl. Organomet. Chem.* **2003**, *17*, 3–8; c) M. Hoch, *Appl. Geochem.* **2001**, *16*, 719–743.
- [9] a) L. Pellerito, L. Nagy, *Coord. Chem. Rev.* **2002**, *224*, 111–125; b) M. Nath, S. Pokharia, R. Yadav, *Coord. Chem. Rev.* **2001**, *215*, 99–149.
- [10] S. Li, F. Chen, Y. Zhou, J. Wang, H. Zhang, J. Xu, *Chem. Commun.* **2009**, 4179–4181.
- [11] S. Derossi, L. Brammer, C. A. Hunter, M. D. Ward, *Inorg. Chem.* **2009**, *48*, 1666–1677.
- [12] T. Komatsu, H. Sakuragi, J. Nagasawa, F. Nakanishi, *Tetrahedron Lett.* **1998**, *39*, 9451–9454.
- [13] a) M. Kasha, H. R. Rawis, M. A. El-Bayoumi, *Pure Appl. Chem.* **1965**, *11*, 371–392; b) K. Y. Burshtein, A. A. Bagatur'yants, M. V. Alfimov, *Chem. Phys. Lett.* **1995**, *239*, 195–200.
- [14] a) Y. Hong, J. W. Y. Lam, B. Z. Tang, *Chem. Commun.* **2009**, 4332–4353; b) Y. Hong, J. W. Y. Lam, B. Z. Tang, *Chem. Soc. Rev.* **2011**, *40*, 5361–5388; c) A. Qin, J. W. Y. Lam, B. Z. Tang, *Prog. Polym. Sci.* **2012**, *37*, 182–209.
- [15] Selected examples of AIE chemosensors bearing two or more target binding sites: a) H. Shi, J. Liu, J. Geng, B. Z. Tang, B. Liu, *J. Am. Chem. Soc.* **2012**, *134*, 9569–9572; b) X. Wang, J. Hu, T. Liu, G. Zhang, S. Liu, *J. Mater. Chem.* **2012**, *22*, 8622–8628; c) G. Huang, G. Zhang, D. Zhang, *Chem. Commun.* **2012**, *48*, 7504–7506; d) N. Liu, S. Song, D. Li, Y. Zheng, *Chem. Commun.* **2012**, *48*, 4908–4910; e) Y. Liu, C. Deng, L. Tang, A. Qin, R. Hu, J. Z. Sun, B. Z. Tang, *J. Am. Chem. Soc.* **2011**, *133*, 660–663.
- [16] W. Wang, N.-B. Wong, W. Zheng, A. Tian, *J. Phys. Chem. A* **2004**, *108*, 1799–1805.